COMPUTATIONAL AND EXPERIMENTAL MICROSTRUCTURE CHARACTERIZATION OF SELECTIVE LASER MELTED IN 625

Mihaela Raluca CONDRUZ[1], Gheorghe MATACHE[2], Alexandru PARASCHIV[3]

Microstructural and phase development investigations were done on IN 625 superalloy manufactured by selective laser melting. The process parameters used generated a level of 99.18% measured relative density as a result of internal defects presence (pores, unmelted particles, microcracks). By metallography method an average level of 0.87% porosity was measured. Thermodynamic calculations showed the possibility of multiple phase development, while experimentally only the γ phase emerged during solidification of IN 625. The experimentally and computational analysis revealed that Nb presents a high tendency to segregate, even at high solidification rates encountered during selective laser melting process.

Keywords: SLM, additive manufacturing, IN 625, microstructure, phase development

1. Introduction

For nearly 9 decades, nickel-based superalloys were considered the most reliable materials when it comes to applications where high temperatures, high stress and corrosive environments are implied (i.e. components for gas turbines). Throughout time, parts made from nickel superalloys were obtained by multiple metallurgical methods (forging, casting, powder metallurgy [1]), but nowadays, the industry is focused on advanced manufacturing techniques such as additive manufacturing (AM) in order to produce complex shaped parts from nickel, aluminum and iron alloys [2].

The main methods used in the field of metallic additive manufacturing are the powder bed fusion processes, like selective laser melting (SLM). SLM process implies the melting of a powder layer with a laser source following up a 3D CAD model, similarly to a laser welding process which allows the complete melting of the powder material [3, 4]. This process has been studied for many years, but until

[1] Scientific Researcher, Romanian Research and Development Institute for Gas Turbines COMOTI, Bucharest, Romania, e-mail: raluca.condruz@comoti.ro
[2] Scientific Researcher, Romanian Research and Development Institute for Gas Turbines COMOTI, Bucharest, Romania, e-mail: gheorghe.matache@comoti.ro
[3] Scientific Researcher, Romanian Research and Development Institute for Gas Turbines COMOTI, Bucharest, Romania, e-mail: alexandru.paraschiv@comoti.ro

today it hasn't been used to its fully potential due to a lack of optimum process parameter selection for different types of powder and different equipment. The final characteristics of the material obtained by SLM are primarily influenced by the feedstock quality and process parameters selection. All these factors can cause many defects in the as-built material. For example, the powder shape, size and distribution can affect the packing factor of powder layer which can cause uneven melted areas. Also, powder porosity (manufacturing process induced porosity) leads to material internal pores, interaction between laser beam and powder can produce balling defects or incomplete powder melting, scanning strategy can influence the stress state of the final part which can lead to layer cracking, delamination or even part shape modification after removing from the base plate [5-12].

IN 625 is a nickel-chromium superalloy developed for manufacturing parts used in harsh environments. It is characterized by a high content of Cr which provides corrosion resistance (by surface formation of Cr_2O_3), while other elements ensure solid solution strengthening (i.e. Mo) or precipitation strengthening (i.e. Nb). During solidification, multiple phases can emerge, but the primary phase developed consists in an austenitic phase – γ matrix (face-centered cubic structure - FCC), followed by secondary phases like γ" phase (Ni_3Nb, a metastable phase with a body centered tetragonal structure - BCT), carbides and multiple topologically closed packed phases (i.e. Sigma, P) caused mainly by segregation of different alloying elements. Also, it must be stated that during operation at high temperatures, the γ" phase can be replaced by deleterious orthorhombic δ phase characterized by the same stoichiometry [4, 13].

Even if most studies are focused on AM of IN 718 superalloy, many research studies were conducted on AM IN 625 as well. It was established that large proportions of powder feedstock with average diameter of 10 μm ($D_{90} \leq$ 10μm) can negatively affect the usability of the material, so it is recommended to use powder with a higher average diameter than 10 μm [14]. Regarding the material microstructure it was stated that AM IN 625 microstructure is characterized by very fine dendritic structures composed of equiaxed grain colonies formed at the surface of the melt pool due to rapid cooling, followed by large columnar grains that grow epitaxial near the fusion line and can extend on multiple layers due to re-melting of previous deposited layers [15-21]. Most studies showed that during rapid solidification, mainly the γ phase is formed in IN 625 followed by emergence of small Nb-rich MC carbides (10-50 nm) in dendrite cores [15], but except these two phases others phases like γ" precipitates, Cr-rich $M_{23}C_6$ carbides are formed by solid phase transformation during heat treatments [15-19]. Typical AM material defects were reported in the literature for IN 625, defects like pores due to unmelted powder particles, lack of fusion defects and balling [15-21]. Different values were reported for the material relative density,

for example Gao et. al. [22] reported a relative density of 99.7% for electron beam melting manufactured IN 625, while Terris et. al. [23] obtained relative densities between 95.5 – 99.8%. The goal of the present study was to evaluate the microstructural and phase development in case of IN 625 manufactured by SLM, using computational and experimental means.

2. Experimental procedure

2.1 Materials and procedures

Gas atomized powder of IN 625 superalloy, provided by LPW Technology Ltd., was used for experimental investigations (particle size distribution D_{10} = 20±2µm, D_{50} = 30±5µm, D_{90} = 45±5µm). Prismatic specimens of 15 x 15 x 30 mm^3 (L x l x h) built in vertical position as shown in Fig. 1 were manufactured with a Lasertec 30SLM machine (1st generation) using the process parameters presented in Table 1.

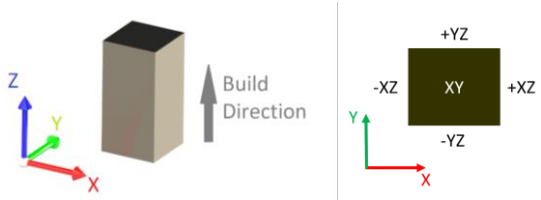

Fig. 1. Schematic representation of the specimens manufactured

Table 1.

Manufacturing process parameters

	Layer thickness 40 µm				
	Laser current [mA]	Exposure time [µs]	Distance between points [µm]	Repetitions	Focus [mm/100]
Support points	2000	200	20	1	0
Support material	700	60	30	1	0
Contour	1500	20	10	1	0
Sample structure network	2000	200	20	1	0
Hatch	2000	40	40	1	120

After manufacturing, the specimens were mechanically removed from the machine building plate. Microstructural investigations were performed on as-built specimens and after they were metallographically prepared by grinding, polishing and etching with an etchant made of 10 ml HNO_3, 10 ml CH_3COOH, 15 ml HCl and 5 drops of glycerin. Microstructural and microcompositional investigations were performed using the scanning electron microscope (SEM – FEI Inspect F50) and energy dispersive spectrometry method (EDS). In order to assess the porosity

level an analysis was realized by processing SEM images using the Scandium software. A binarization technique was achieved by adjusting the brightness and contrast to highlight the pores; further the images were converted to a 16-bit greyscale format followed by conversion into black and white threshold images. The porosity analysis was realized on 10 micro areas (1.9 mm^2) in different cross sections of the un-etched specimens.

The phases development assessment was performed both experimentally by X-ray diffraction and computationally by thermodynamic calculations using Pandat™ (Computherm LLC, PanNi2018_TH database). These investigations aimed to accurately determine which phases emerged during the rapid solidification of IN 625. Using Pandat™ it was also analyzed the solidification path for equilibrium and non-equilibrium conditions (Lever and Scheil models). As input data for thermodynamic calculations different chemical compositions were used: the chemical composition of IN 625 powder from the technical specification and the chemical composition of IN 625 material experimentally determined by EDS. The specimen density was determined by Archimedes method using an analytical balance Pioneer PX223 (Ohaus) equipped with a density kit, according ISO 3369 standard.

2.2 Results and discussions

Microstructural investigations and phase development analysis

At lower magnification (200x), it can be observed that the microstructure of the SLM manufactured IN 625 is similar with the microstructure of a laser welded material - Fig. 2. Regarding the development of the microstructure, it can be said that is was formed by heterogeneous nucleation mechanism at the interface of powder particle – melted material and by epitaxial and competitive growth. Due to a high ratio between undercooling rate and solidification speed, the microstructure presents different morphologies.

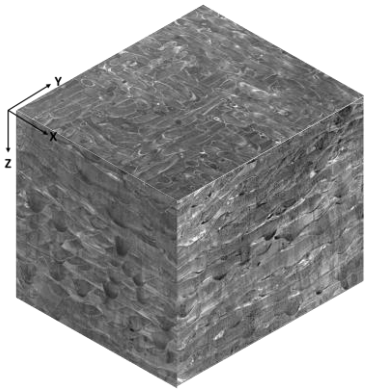

Fig. 2. 3D representation of a specimen microstructure based on SEM images

Dendritic columnar along with dendritic cellular morphologies were observed. Grains formed with different orientations appeared as a sign of competitive growth, along with large crystals arranged on multiple layers as a sign of epitaxial growth. In SEM images the deposited layer boundaries, the heat affected area - HAZ (element found also in welded structures) and melted pool traces can be distinguished – Fig. 3.

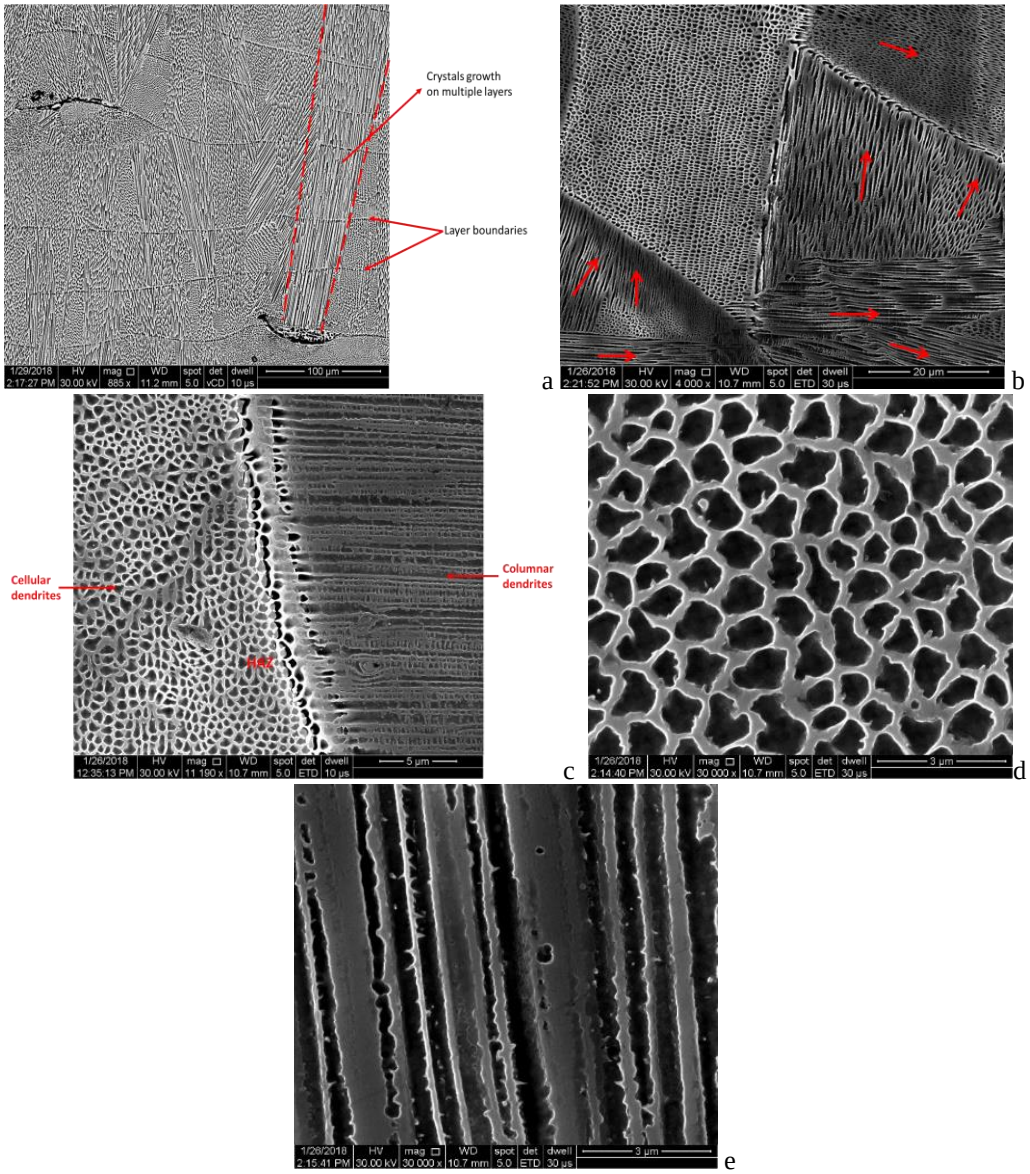

Fig. 3. SEM images with IN 625 microstructure: a) epitaxial growth of crystals; b) competitive growth of crystals; c) different morphologies of dendrites; d) cellular dendrites; e) columnar dendrites

The phase analysis was done by thermodynamic calculations using *Pandat*™ and experimental measurements. The chemical compositions used for thermodynamic calculations are presented in Table 2. The solidification path for both equilibrium and non-equilibrium conditions was analyzed using the experimentally determined chemical composition as presented in Fig. 4.

Table 2.

Chemical compositions of IN 625 used for thermodynamic calculations

	Al	C	Co	Cr	Fe	Mo	Nb + Ta	Ti	Ni
Technical specification	<0,4	<0,1	<1,0	20-23	3-5	8-10	3,15-4,15	<0,4	Bal.
Experimentally	0,1	0,02	0,1	21,6	4,0	9,0	3,5	0,17	Bal.

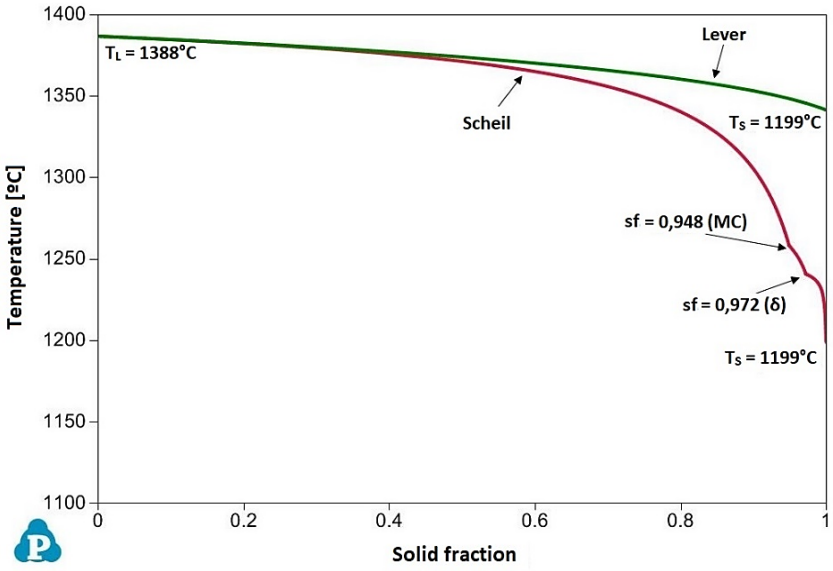

Fig. 4. Solidification path of IN 625 alloy in equilibrium and non-equilibrium conditions

The diagram presented in Fig. 6 shows the same liquidus temperature (T_L = 1388°C) for equilibrium – Lever and non-equilibrium – Scheil conditions, but different solidus temperatures (T_S) are predicted. For equilibrium conditions a T_S = 1341°C was predicted while in non-equilibrium conditions, the T_S was underestimated (T_S = 1199°C). The difference between the two models is caused mainly because the software predicts only the formation of the γ phase in equilibrium conditions while in case of non-equilibrium conditions the software predicts the formation of multiple solid fractions, like δ (at a solid fraction of 0.971, respective T = 1240ºC) and primary carbides MC (at a solid fraction of 0.948, respective T = 1258ºC). Moreover, using Scheil method it can be predicted the distribution of the alloying elements near the solidification front (Fig. 5) in order to observe the segregation tendency during solidification.

In case of IN 625 it was observed that Nb presents the highest tendency to segregate at the end of the solidification process. Taking into account this observation, the influence of Nb content on the transformation temperatures was analyzed. For this evaluation, the Nb content was selected based on the range provided by the composition from the technical documentation. The values used were: 3.15%wt. Nb, 3.3% wt. Nb, 3.5% wt. Nb, 3.75% wt. Nb, 4% wt. Nb, 4.15% wt. Nb. The results of the analysis are presented in Fig. 6.

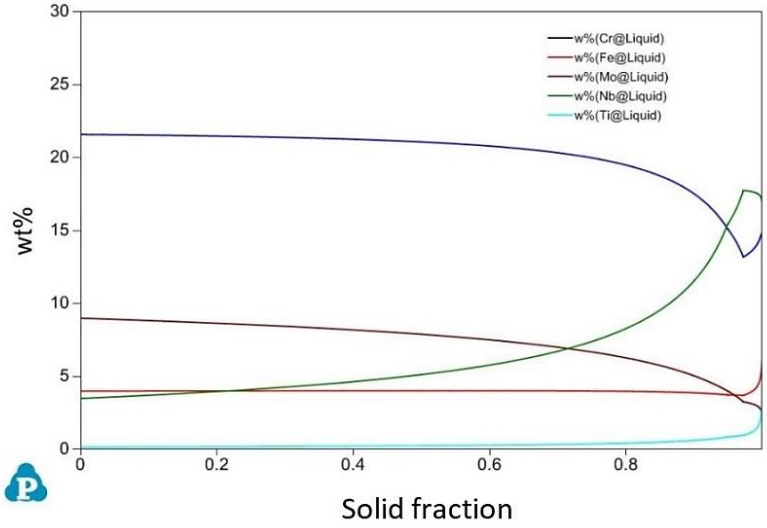

Fig. 5. Prediction of alloying elements distribution near the solidification front

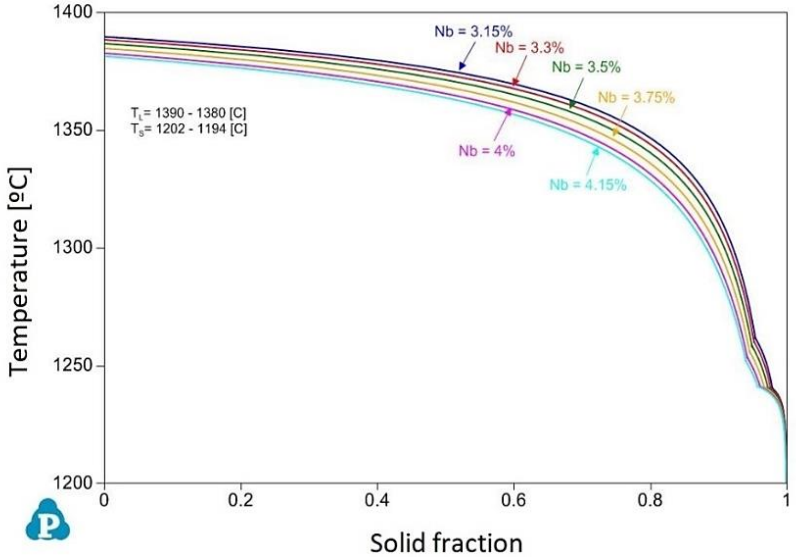

Fig. 6. The influence of Nb content on the transformation temperatures (Scheil method) in IN 625

It was noticed that small variation of Nb content influence the transformation temperatures. Increasing the Nb content reduces the T_L and T_S of the alloy, reduces the temperature range where the MC carbides are formed and reduces the temperature at which the δ is formed. By using the chemical composition of the IN 625 powder in Pandat™ software, there were predicted the phases that can develop in the material during solidification and cooling. Pandat™ predicts a high fraction of γ phase at high temperature. As the temperature decreases other phases could be formed (σ, δ, P, $M_6C \rightarrow M_{23}C_6$). The fraction of predicted phases as a function of temperature is presented in Fig. 7.

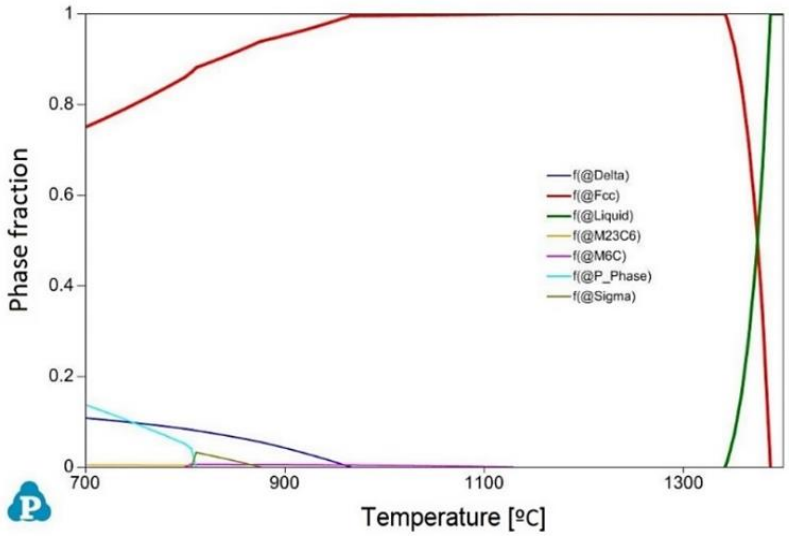

Fig. 7. Diagram with phase fractions developed during the solidification of IN 625 superalloy

By SEM investigations analysis, multiple phase morphologies were observed in SLM manufactured IN 625 – Fig. 8. Even if different morphologies were observed in SEM images, based on EDS analysis it was concluded that only one phase was developed during the rapid solidification of AM IN 625, namely the γ phase.

Pandat™ predicts a fraction of 99.6% γ phase after solidification at 1000°C. The prediction is in good agreement with the X-ray diffraction results on as-built specimens that show that the dominant phase is γ phase (FCC), while other possible minor phases are under 1%.

The morphological differences encountered were caused by the combination of process parameters and scanning strategy, dendrite growth direction, melting temperature, remelting of multiple layers and high solidification rates.

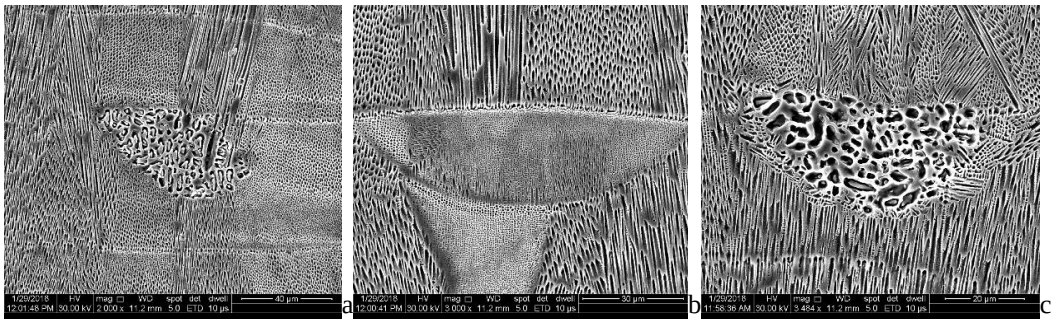
a b c

Fig. 8. Morphologies encountered in IN 625

An EDS analysis was performed on equiaxed dendrite core and in interdendritic regions in order to evaluate the elemental segregation. Using the EDS results (Table 3), the partition coefficient K_s was calculated with eq. (1). The $K_{S(i)}$ partition coefficient represents the tendency of the alloying element to segregate either in the dendrite cores ($K_{S(i)}>1$) or in the interdendritic areas ($K_{S(i)}<1$).

$$K_{s(i)} = \frac{C_{c(i)}}{C_{I(i)}} \tag{1}$$

where: $K_{s(i)}$ – repartition coefficient of element i;

$C_{c(i)}$ – concentration of the element (i) in cellular dendrite cores;

$C_{I(i)}$ – concentration of element (i) in interndritic areas.

Table 3

Medium values of the chemical composition determined by EDS

	C	Al	Si	P	Nb	Mo	Ti	Cr	Mn	Fe	Co	Ni
Dendrite core	0.05	0.08	0.05	0.02	3.75	9.29	0.18	21.75	0.01	3.885	0.1	Bal.
Interdendritic area	0.08	0.09	0.05	0.02	4.92	11.8	0.18	21.11	0.01	3.73	0.1	Bal.

The experimental results were correlated with the results from simulation results and it was concluded that even in case of rapid solidification Nb and Mo segregates in the interdendritic areas ($K_{S\,Nb} = 0.76$, $K_{S\,Mo} = 0.79$).

Density and porosity analysis

Significant differences regarding the density of the specimens were not observed, the average value of material density being 8.42 g/cm^3 compared with the theoretical density of IN 625 determined by calculations using the chemical composition of the powder material which is 8.49 g/cm^3. Using the presented process parameters and the measurements a relative density of the material of 99.18% was calculated. The low degree of densification was caused by the process induced internal defects, like pores, lack of fusion and microcracks.

It was observed that unmelted powder particles were entrapped in big pores. Theoretically, based on the density measurements, the material should exhibit an average of 0.82% porosity level.

The experimentally measured porosity level was in the range of 0.24% – 1.5% (average value 0.87%). The differences are caused by the uneven distribution of internal pores, areas with multiple pores were encountered along with areas with a reduce degree of porosity – Fig. 9. Future investigations should be realized in order to define proper process parameters that can be used in order to obtain denser material.

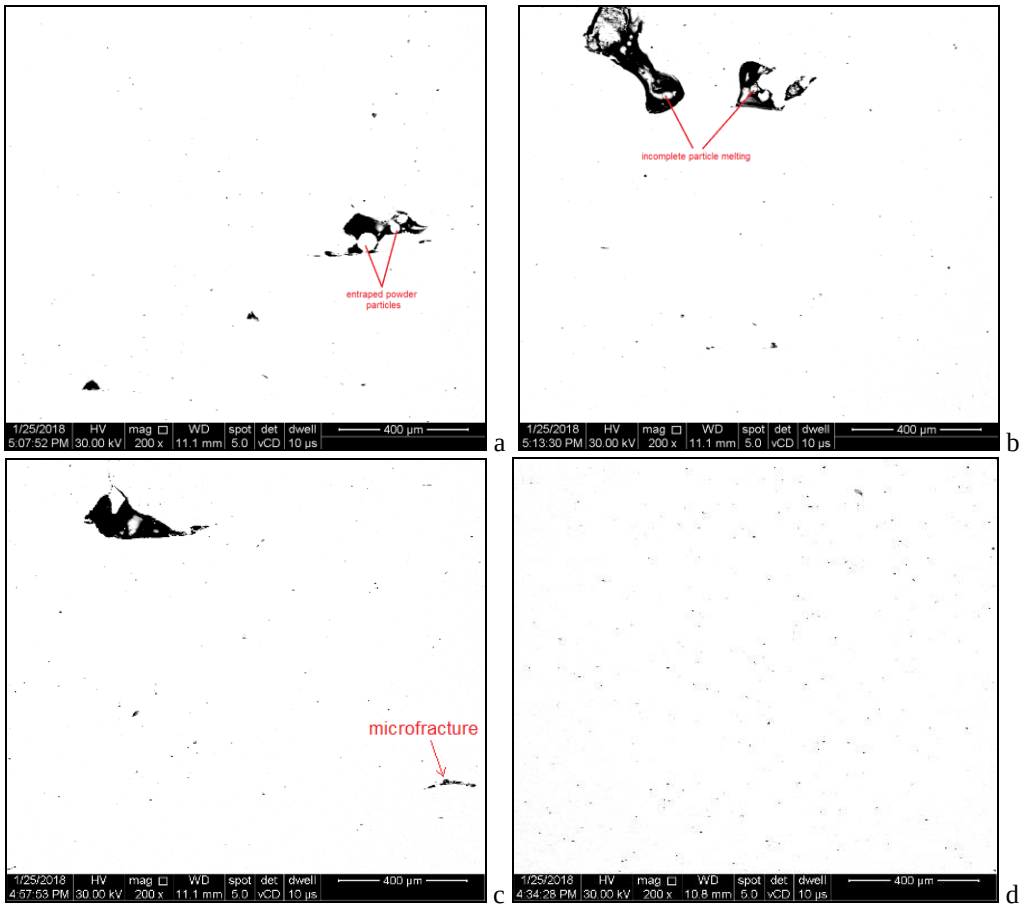

Fig. 9. Binarized SEM images used for porosity evaluation

3. Conclusions

The present work was carried out on IN 625 superalloy manufactured by SLM. The results showed that the process parameters used induced surface material defects – balling caused by material boiling and splash of the melt pool.

Due to presence of many internal defects (unmelted powder particles, pores, microfractures) the material have a degree of densification of only 99.18%. The experimentally determined porosity level was in the range of 0.24% – 1.5% (average value 0.87%) depending on the cross-section investigated. The pores formed during the process are randomly distributed all over the specimens and exhibits multiples shapes. It was observed that unmelted powder particles were entrapped in big pores.

The microstructure of SLM manufactured IN 625 is similar with the microstructure of a laser welded material, with columnar and cellular dendritic morphologies. By thermodynamic calculations it was predicted that multiple phases can emerge during material solidification. It was experimentally determined that due to high solidification rate mainly the γ phase was formed. It was also observed that Nb presents a high tendency to segregate, even at high solidification rates encountered during SLM. Further studies will be conducted in order to optimize the process parameters that can be used in order to obtain denser material and to investigate their influence on the mechanical properties of SLM manufactured IN 625.

Acknowledgement

Project funded by Research and Innovation Ministry through the Program 1 – Development of the National Research System-Subprogram 1.2 – Institutional Performance – Projects for Excellence Financing in RDI Contract no. 3PFE/2018. The authors thank to Dr. Eugeniu Vasile from University POLITEHNICA of Bucharest for the XRD verification.

R E F E R E N C E S

[1] *Cojocaru M., Tudose F.,* Synthesis of Nickel Aluminides by Mechanical Alloying in Ball Mills, UPB Sci.Bul., Series B, 78 (4):181-192, 2016

[2] A. Mauduit, S. Pillot, H. Gransac, Study of the Suitability of Aluminum Alloys for Additive Manufacturing by Laser Powder-Bed Fusion, UPB Sci. Bull., Series B., 79 (4):219-238, 2017

[3] *Gu D,* Laser Additive Manufacturing of High-Performance Materials, Springer-Verlag Berlin Heidelberg, 2015

[4] *DuPont JN, Lippold JC, Kiser SD,* Welding Metallurgy and Weldability of Nickel-base Alloys, John Wiley & Sons, Inc., New Jersey, 2009

[5] *Kruth JP, Dadbakhsh S, Vrancken B, Kempen K, Vleugels J, Van Humbeeck J,* Additive Manufacturing of Metals via Selective Laser Melting: Process Aspects and Material Developments. In: Srivatsan TS, Sudarshan TS (eds) Additive Manufacturing: Innovations, Advances, and Applications. CRC Press, New York, pp 69-100, 2016

[6] *Sames WJ, List FA, Pannala S, Dehoff RR and Babu SS,* The metallurgy and processing science of metal additive manufacturing, Int Mat Rev 61(5):315-360, 2016

[7] *Siddiqui SF, Fasoro AA, Gordon AP,* Selective laser melting (SLM) of Ni-based superalloys: A mechanics of materials review. In: Badiru AB, Valencia VV, Liu D (eds) Additive

Manufacturing Handbook: Product Development for the Defense Industry. CRC Press, New York, pp. 225-250, 2017

[8] *Bourell D, Kruth JP, Leu M, Levy G, Rosen D, Beese AM, Clare A*, Materials for additive manufacturing, CRRP Annals – Manufacturing Technology 66:659-681, 2017

[9] *Collins PC, Birce DA, Samimi P, Ghamarian I, Fraser HL*, Microstructural Control of Additively Manufactured Metallic Materials, Annu Rev Mater Res 46:63-91, 2016

[10] *DebRoy T, Wei HL, Zuback JS et al.*, Additive manufacturing of metallic components – Process structure and properties, P Mat Sci 92:112-224, 2018

[11] *Kruth JP, Badrossamay M, Yasa E, Deckers J, Thijs L, Van Hymbeeck J*, Parts and material properties in selective laser melting of metals, Proceeding of 16th International Symposium on Electromachining (ISEM – XVI), Shanghai Jiao Tong University Press, Shanghai, China, 2010

[12] *Prashanth KG, Scudino S, Maity T, Das J and Eckert J*, Is the energy density a reliable parameter for materials synthesis by selective laser melting? Mat Res Let, 5(6): 386-390, 2017

[13] *Donachie MJ, Donachie SJ*, Superalloys: A Technical Guide 2nd ed. ASM International, Ohio, 2002

[14] *Pless C, Jothi S*, Influence of powder characteristics and additive manufacturing process parameters on the microstructure and mechanical behavior of Inconel 625 fabricated by Selective Laser Melting, Add Ma 24: 419-431, 2018

[15] *Marchese G, Lorusso M, Parizia S, Bassini E et al.*, Influence of heat treatments on microstructure evolution and mechanical properties of Inconel 625 processed by laser powder bed fusion, Mat Sci Eng A 729: 64-75, 2018

[16] *Li C, Guo YB, Zhao JB*, Interfacial phenomena and characteristics between the deposited material and substrate in selective laser melting Inconel 625, J Mat Pro Tec 243:269-281, 2017

[17] *Li S, Wei Q, Shi Y, Zhu Z, Zhang D*, Microstructure Characteristics of Inconel 625 Superalloy Manufactured by Selective Laser Melting, J Mar Sci Tec 31:946-952, 2015

[18] *Li C, White R, Fang XY, Weaver M, Gu YB*, Microstructure evolution characteristics of Inconel 625 alloy from selective laser melting to heat treatment, Mat Sci Eng A 705:20-31, 2017

[19] *Amato KN, Hernandez J, Murr LE, Martinez E, Gaytan SM, Shindo PW*, Comparison of Microstructure and Properties for a Ni-Base Superalloy (Alloy 625) Fabricated by Electron and Laser Beam Melting, J Mat Sci Res 1(2): 3-41, 2012

[20] *Hu YL, Lin X, Zhang SY, Jiang YM, Lu XF, Yang HO, Huang WD*, Effect of solution heat treatment on the microstructure and mechanical properties of Inconel 625 superalloy fabricated by laser solid forming, J Al Com 767:330-344, 2018

[21] *Hu YL, Lin X, Lu XF, Zhang SY, Yang HO, Wei L, Huang WD*, Evolution of solidification microstructure and dynamic recrystallization of Inconel 625 during laser solid forming process, J Mater Sci 55:15650-15666, 2018

[22] *Gao Y, Zhou M*, Superior Mechanical Behavior and Fretting Wear Resistance of 3D-Printed Inconel 625 Superalloy, Appl Sci 8, 2439, 2018

[23] *Terris T, Adamski F, Peyre P, Dupuy C*, Influence of SLM process parameters on Inconel 625 superalloy samples, Proceedings of Lasers in Manufacturing Conference 2017, Munchen, Germany, https://www.wlt.de/lim/Proceedings2017/Data/PDF/Contribution110_final.pdf Accessed at 03.05.2019